

Accepted Manuscript

The age of undeformed dacite intrusions within the Kolaka fault zone, SE Sulawesi, Indonesia

L.T. White, R. Hall, R.A. Armstrong

PII: S1367-9120(14)00357-5

DOI: <http://dx.doi.org/10.1016/j.jseaes.2014.08.014>

Reference: JAES 2055

To appear in: *Journal of Asian Earth Sciences*

Received Date: 26 February 2014

Revised Date: 5 August 2014

Accepted Date: 9 August 2014

Please cite this article as: White, L.T., Hall, R., Armstrong, R.A., The age of undeformed dacite intrusions within the Kolaka fault zone, SE Sulawesi, Indonesia, *Journal of Asian Earth Sciences* (2014), doi: <http://dx.doi.org/10.1016/j.jseaes.2014.08.014>

This is a PDF file of an unedited manuscript that has been accepted for publication. As a service to our customers we are providing this early version of the manuscript. The manuscript will undergo copyediting, typesetting, and review of the resulting proof before it is published in its final form. Please note that during the production process errors may be discovered which could affect the content, and all legal disclaimers that apply to the journal pertain.



The age of undeformed dacite intrusions within the Kolaka fault zone, SE Sulawesi, Indonesia

L. T. White¹, R. Hall¹, R. A. Armstrong²

1. Southeast Asia Research Group, Department of Earth Sciences, Royal Holloway University of London, Egham, Surrey, TW20 0EX
2. Research School of Earth Sciences, The Australian National University, Canberra, Australia, 0200

ABSTRACT

We present petrologic, geochemical and U-Pb sensitive high resolution ion microprobe (SHRIMP) data from previously undocumented dacite intrusions from the SE Arm of Sulawesi. The dacites occur in a strand of a major fault (the Kolaka Fault) that crosses the SE Arm of Sulawesi and northern Bone Bay. U-Pb SHRIMP dating shows the “Kolaka Dacite” yields zircon grains and overgrowths that range between ca. 4 and 7 Ma, indicating active magmatism in SE Sulawesi at this time. The youngest age population (4.4 ± 0.2 Ma) from this range is interpreted to be the maximum crystallization age for the dacite. The Kolaka Dacite is undeformed, and so potentially intruded during or after movement within a strand of the Kolaka Fault. The dacites may have otherwise been emplaced passively along existing foliation planes in the country rock schist. Additional U-Pb data were collected from inherited zircons, yielding ages between 8 Ma and 1854 Ma. We consider that these inherited zircons are xenocrysts, derived from either (1) a partially melted protolith and/or (2) xenocrysts assimilated during ascent of the magma. In either case, the inherited zircons record the age of the basement rocks beneath this part of SE Sulawesi. These inherited zircon cores show that the SE arm of Sulawesi is underlain by Proterozoic or younger material, validating earlier ideas that the crust here was derived from Gondwana.

Keywords: Sulawesi, Kolaka, SHRIMP, geochronology, structure, geochemistry

1. INTRODUCTION

Sulawesi represents a region of collision, where west Sulawesi (a rifted margin of Sundaland), the Sula Spur (Australian margin) and Sulawesi's North Arm (volcanic arc) collided during the Late Oligocene-Early Miocene (e.g. Audley-Charles 1974; Hamilton 1979; Sukamto and Simandjuntak 1983; Hall 1996, 2002; 2012). This collision, and subsequent phases of crustal extension and strike-slip faulting led to the island's distinctive K-shape. The arms of the island are commonly divided into the: (1) North Sulawesi Volcanic Province (volcanic arc rocks), (2) Western Sulawesi Province (arc rocks and continental basement), (3) Central Sulawesi Metamorphic Belt, (4) East Sulawesi Ophiolite, and (5) other micro-continental fragments (East Arm and Buton) (Parkinson 1998a; Elburg et al. 2003; van Leeuwen et al. 2007; Cottam et al. 2011) (Figure 1). All of these terranes are cut by major strike-slip faults (e.g. the Walanae Fault System (van Leeuwen 1981; Sukamto 1982; Berry and Grady 1987; Jaya and Nishikawa 2013), the Gorontalo Fault (Katili 1978), the Matano Fault (Hamilton 1979; Silver et al., 1983a,b), the Palu-Koro Fault (Katili 1970; Hamilton 1979; Silver et al. 1983a,b), the Lawanopo Fault (Hamilton 1979), and the Kolaka Fault (Simandjuntak et al. 1984; Surono 1994) (Figure 1). In this paper, we focus on the geology of the SE Arm of Sulawesi and report field relationships, petrology, geochemistry and geochronology data from a previously undocumented dacite intrusion found within a strand of the Kolaka fault zone.

1.1 The Southeast Arm

Much of the SE Arm of Sulawesi is unpopulated, mountainous and heavily forested, meaning that very little geological work has been undertaken in the area. From the mapping that has been conducted, we know that the SE Arm is dominated by low to high-grade schists, as well as

ultramafic and sedimentary rocks (Hamilton 1979; Rusmana et al. 1993; Simandjuntak et al. 1984; 1994; Suroño 1994) (Figure 2). The schists have been interpreted as part of the basement and were originally considered to have a Palaeozoic age (Suroño 1994). This age was assigned because the schists are cross-cut by aplites that were considered to have been intruded during the Permian or Carboniferous (Suroño 1994; 1998). However, the reason that the aplites were assigned Permian to Carboniferous ages is not documented. Given the absence of age constraints on the cross-cutting aplites, it is equally likely that the schists of the SE Arm are related to either the Early Cretaceous Pompangeo Schist of Central Sulawesi Province (Parkinson 1998b), or the schists of the Bantimala Metamorphic Complex (Wakita et al. 1996). They could also be related to none of these; a Cenozoic age is feasible.

In the SE Arm, Triassic sediments are unconformably overlain by Jurassic to Cretaceous carbonates (Tetambaha Formation), Eocene shallow marine carbonates (Tampakura, Lerea and Tamborasi formations) and Oligocene deposits of melange (Suroño 1994). All of these units have faulted contacts with ultramafic rocks which are rightly or wrongly considered to be part of the East Sulawesi Ophiolite. These rocks are unconformably overlain by the Neogene Celebes Molasse and recent alluvium (Hamilton 1979; Silver et al. 1983b; Suroño 1994).

The SE Arm of Sulawesi is cross-cut by two major strike-slip fault systems. The northern-most fault is referred to as the Lawanopo Fault System, and the southern-most fault is named the Kolaka Fault (Hamilton 1979; Simandjuntak et al. 1984, 1994; Suroño 1994) (Figure 1). These faults are identified on aerial and satellite imagery as straight, northwest trending features (e.g. coastlines and cliffs). However, as the strike of these faults is parallel to the regional structural grain, their offset is uncertain (Hamilton 1979), but are commonly interpreted to have a sinistral sense of movement, most likely because of the apparent offset of parts of the SE Arm. Both of these faults are considered to extend from onshore the SE Arm of Sulawesi into Bone Bay. Wide fault zones are

observed in reflection seismic data along strike from the fault zones on land (Camplin and Hall, 2013; 2014). These faults are considered to have been active during the Plio-Pleistocene (Surono 1994) or during the Middle to Late Miocene to recent times (Camplin and Hall 2013; 2014) according to cross-cutting relationships and deformation of sediments within Bone Bay. However, there are no isotopic geochronological data available to establish when these faults initiated, so our knowledge of the timing of fault displacements depends on limited biostratigraphic data from deformed sedimentary sequences, or indirect estimates of ages interpreted from offshore seismic data (Camplin and Hall, 2013; 2014). This limits our understanding of the timing and duration of tectonic events in this region. We report new geological and U-Pb geochronological data from an undeformed dacite found within a strand of the Kolaka fault zone, close to the faulted contact between the undated schists and ultramafic rocks (Figure 2).

2. SAMPLES AND METHODOLOGY

Exposures of flow-banded, porphyritic dacite were found in two newly excavated road cuts between Kolaka and Lasusua, along the west coast of Bone Bay (Figure 2 and 3). The first sample ES12-21 was collected from Latitude: 3.612714°S / Longitude: 120.975189°E. The second sample ES12-22 was collected Latitude: 3.637220°S / Longitude: 120.996184°E (Figure 2). The dacites intrude poly-deformed schist at both outcrops (Figure 3). The contact with the schists exhibits chilled margins and is dominantly very steep (066°/70°S to 136°/86°NE) and the overall strike of the contact is ~140°. The orientation of flow-banding is predominantly vertical, and shares the same orientation as the dominant schistosity (106°/90° to 132°/89°NE) of the country rock which it has intruded. As the schistosity in the country rock was folded prior to the dacite intrusion there are some irregularities in the orientation of the contact between the two units and the flow banding in the dacite. We refer to these intrusive rocks as the Kolaka Dacite.

The vertical contact between the Kolaka Dacite with the schist as well as chilled margins indicate that these rocks probably intruded as thick (~30m) dykes (e.g. Figure 3a) in a hypabyssal setting. We did not observe a faulted contact between the dacites and the country rock, but our observations were made very near to where a faulted contact is drawn on the 1:250,000 geological map of the region between the schist and ultramafic rocks (Simandjuntak et al., (1994); Figure 2). Lineaments identified from Shuttle Radar Topographic Mission (SRTM) data (Figure 2) indicate that the Kolaka Fault extends into Bone Bay south of the dacite outcrops, where the fault is observed further offshore in seismic reflection and multibeam bathymetry data (Camplin and Hall 2013; 2014). However, other major lineaments are obvious in the SRTM data in the region where the dacite was observed (Figure 2).

The two samples (ES12-21 and ES12-22) were collected from exposures 3.5 km apart and both have the same appearance in hand specimen and thin section. They are composed of millimetre to centimetre scale crystals of hornblende and felsic xenoliths within a fine, light-grey matrix composed of plagioclase, quartz and hornblende as well as minor biotite (Figures 3 and 4). An examination of thin sections shows that the centimetre scale hornblende crystals are in fact clusters of smaller hornblende crystals (glomerocrysts) within a finer grained groundmass (Figure 4b and 4c). Although not observed in thin section, we identified trace amounts of magnetite, fluorite, apatite, zircon, gold and molybdenum during the heavy mineral separation process (see Section 2.2).

2.1 Geochemistry

Both samples (ES12-21 and ES12-22) were crushed into 2-5 cm³ pieces. The crushed aggregate was washed to remove any potential contaminants from the jaw crusher and left to dry before being pulverised to a fine-powder using a tungsten carbide mill. The powder that was less than 250 µm was collected using a sieve and disposable nylon mesh. Most of the material was sunk in high-

density liquids to separate zircon, but an aliquot of the powder was taken prior to this step to be milled further and made into glass disks and pellets for whole rock major and trace element geochemical analyses. These analyses were conducted using a Panalytical Axios WDS XRF spectrometer at Royal Holloway, University of London.

2.2 Geochronology

Zircons were extracted from heavy liquid concentrates and a Frantz magnetic separator before being hand picked and set in a 25 mm epoxy disk along with the Temora-2 U-Pb zircon standard (Black et al. 2004). The mount was polished to expose the mid-sections of the grains and was examined with an optical microscope and photographed under transmitted and reflected light. All zircons were then imaged with a Robinson Cathodoluminescence (CL) detector fitted to a JEOL JSM 6610-A scanning electron microscope (SEM) at the Research School of Earth Sciences, The Australian National University (ANU).

A sensitive high resolution ion microprobe with reverse geometry (SHRIMP RG) at the ANU was used to analyze the U, Th and Pb isotopic species of zircons that were free of inclusions and cracks. The SHRIMP measurements were calibrated using the SL13 uranium concentration standard (U = 238 ppm) at the beginning of the analytical session. One Temora-2 U-Pb standard (417 Ma) (Black et al., 2004) was measured for every three unknown zircons. The data obtained from SHRIMP-RG was reduced using the SQUID 2 program (<http://sourceforge.net/projects/squid2/files/>) and interrogated further with Isoplot (Lugwig 2003).

In this paper, ages that are <900 Ma are reported using the ^{207}Pb corrected $^{206}\text{Pb}/^{238}\text{U}$ system because of the errors that are associated with low yields of ^{204}Pb , ^{207}Pb and ^{208}Pb from relatively young zircons. This method effectively assumes that each analysis is a mixture of radiogenic and

common lead, and this is unmixed from the measured $^{207}\text{Pb}/^{206}\text{Pb}$ (Muir et al. 1996). All ages older than 900 Ma are reported using the ^{204}Pb corrected $^{207}\text{Pb}/^{206}\text{Pb}$ ratio.

3. RESULTS

3.1 Geochemistry

The whole rock major and trace element data for both samples are shown in Table 1. These data show that both samples plot within the dacite field of the IUGS total alkali vs. silica diagram (LeBas and Streckeisen 1991) (Figure 5) and have a medium- to high-potassium, calc-alkaline composition. The trace element data shows that the Kolaka Dacite is enriched in all elements relative to average primitive mantle compositions (Palme and O'Neill 2003), with relatively high amounts of Cs, Rb, Th, U, Pb and Sr, and lower amounts of Nb, Ta, La, Nd, Sm, Hf, Zr, Y and Yb (Figure 5). The amount of SiO_2 (68-70%), MgO (1.86-1.93%) and TiO_2 (0.49%), as well as the relative abundance of Pb and Sr and relative depletion of Nb indicate that these have what many consider a subduction signature (e.g. Elburg and Foden 1999a;b; Elburg et al. 2003).

3.2 Geochronology

3.2.1 Kolaka Dacite Sample 1 (“ES12-21”)

The zircon grains in ES12-21 yielded ages between 4.0 (± 0.2) Ma and 621 (± 7.0) Ma, with a cluster of ages between 4.0 and 8.5 Ma (Supplementary File 1a). This sample recorded ^{204}Pb counts between 0.00 and 0.19, $^{207}\text{Pb}/^{206}\text{Pb}$ ratios between 0.052 and 0.189. The few zircon grains that recorded $^{207}\text{Pb}/^{206}\text{Pb}$ values >0.1 Ma (Spots 9.1, 14.1 and 14.2) potentially record Pb loss, however, as the counts of ^{207}Pb are low in such young samples (e.g. 1-4 counts per second), there is potentially a high margin of error when analysing these grains. We therefore excluded the results of these samples in our final calculations.

In ES12-21, U and Th concentrations range from 24 to 1103 ppm and 1 to 240 ppm respectively, and Th/U ratios range between 0.01 and 1.00. The ages of <10 Ma were all collected from zircon grains that showed no evidence of an inherited core and overprinting rim, or from the rims of those grains that showed discernable cores (cf. Supplementary File 2). The <10 Ma zircon grains and zircon rims were all collected from relatively dark zones in the CL SEM images (Supplementary File 2). The <10 Ma zircon grains and rims also have low Th/U ratios between 0.01 and 0.34.

3.2.2 Kolaka Dacite Sample 2 (“ES12-22”)

The grains in ES12-22 yielded ages between 4.4 (± 0.1) Ma and 1859 (± 7.0) Ma, with a cluster of ages between 4.4 and 6.6 Ma (Supplementary File 1b). This sample recorded ^{204}Pb counts between 0.00 and 0.52, $^{207}\text{Pb}/^{206}\text{Pb}$ ratios between 0.049 and 0.114. The one grain that recorded a $^{207}\text{Pb}/^{206}\text{Pb}$ value >0.1 Ma (Spot 3.1) is from an older grain (1859 ± 7 Ma) from which such values would be expected due to production of ^{206}Pb as a daughter isotope, so there was no need to omit any results due to problematic zircon grains or individual analyses.

In ES12-22, U and Th concentrations range from 56 to 825 ppm and 4 to 1107 ppm respectively, and Th/U ratios range between 0.02 and 1.47. The ages of <10 Ma were all collected from zircon grains that showed no evidence of an inherited core and overprinting rim, or from the rims of those grains that showed discernable cores (cf. Supplementary File 2). These zones are all relatively dark in CL SEM imagery and have low Th/U ratios between 0.02 and 0.08 (Supplementary File 2).

Previous work has shown that there is often a correlation between uranium concentration and an increase in apparent age in U-Pb measurements of zircons analysed with the SHRIMP (White and Ireland, 2012). This correlation is due to a matrix-effect associated with SHRIMP measurements of radiation-damaged zircon (White and Ireland, 2012). We found no correlation between the apparent

age of the <10 Ma zircons and uranium concentration in either of the samples analysed in this study (Supplementary File 3) so we are confident that age results reported here are robust.

3.2.3 Age of the Kolaka Dacite

The age results obtained for the two samples of the Kolaka Dacite were combined, as relatively few geochronological data were obtained for each sample, and because the petrological, geochemical and geochronological results are essentially identical. We assume that the youngest cluster of ages obtained (ca. 4 – 7 Ma) records the time of crystallisation of these rocks because no other distinct age population was identified (Figure 6). One other <10 Ma age was obtained (ES12-21-16.1: 8.5 ± 0.4 Ma). As this age was only found in one of the samples, we interpret it as an inherited grain. We assume that the results older than 8.5 Ma also represent inherited zircon either derived from: (1) the protolith (i.e. partially melted source rock), or (2) xenoliths entrained into the melt during magma ascent.

As there is no distinct age population identifiable in the youngest cluster of ages there is an issue of whether to *combine or split* the results when attempting to calculate the age of magmatism. . The most conservative approach is to say that the dacite crystallised between 4 Ma and 7 Ma, but this approach does not reflect the relative proportion of ages that were obtained. The weighted mean age of these data is 5.50 ± 0.53 Ma, MSWD = 34, n = 11. The high MSWD value indicates that this apparent age results from more than one age population. To determine the age of distinct populations within the range we used the “unmix age function” (Sambridge and Compston 1994) within Isoplot, following the approach explained by White et al. (2011). To do this we generated a relative probability plot of the results between 0 and 10 Ma. This plot shows that there are four distinct age peaks (Figure 6c). So the unmix age function algorithm was given an input to request it to define the age of four unique age populations. The program was further instructed to select the

approximate age and relative proportion of data points that define the four populations. The unmixed ages reflect the centre of the peaks that were identified on the relative probability plot (Figure 6c) and are reported below:

- 4.4 ± 0.2 Ma (18% of the population of 11)
- 5.0 ± 0.2 Ma (32% of the population of 11)
- 5.8 ± 0.2 Ma (14% of the population of 11)
- 6.5 ± 0.2 Ma (36% of the population of 11)

The crystallization age of the dacite is interpreted to be the youngest age population identified with the unmix age function. The older age peaks likely reflect earlier crystallization of zircons in the same magma chamber that were brought to the surface, potentially within the felsic xenocrysts incorporated in the porphyritic dacite.

4. DISCUSSION

4.1 Geochronology

We observed the Kolaka Dacite at two large road cut exposures within a strand of the Kolaka fault zone (Figure 2 and 3). The U-Pb ages obtained in this study indicate that the dacite had crystallised by 4.2 ± 0.2 Ma. This provides a minimum age for the last phase of deformation of the schist that it intrudes. While we did not observe direct evidence of the dacite intruding along a fault plane, we suspect that its orientation and occurrence within a strand of the Kolaka fault zone (Figure 2) might indicate that faulting had some influence on the emplacement of these rocks. If this were the case, the Kolaka Fault was active at different times between ca. 4.2 Ma to the present day (considering the deformation of seafloor features in Bone Bay: Camplin and Hall 2013; 2014). An alternative explanation is that the Kolaka Dacite passively intruded along an earlier formed fabric, either a regional basement fabric or along more localised foliations in the country rock schist.

In addition to establishing the crystallisation age of the Kolaka Dacite magma, we also obtained several analyses of inherited zircon grains, rims and cores. We interpret these to be xenocrysts either inherited from a source protolith, or grains assimilated from surrounding wall rocks during ascent of the magma. Although only a limited number of analyses of inherited zircons were obtained from each sample, these provide an insight into the nature and age of the basement rocks. Our results indicate that zircon growth occurred between 8-25 Ma, 60-100 Ma, 130-180 Ma, 210-280 Ma, 300-320 Ma as well as at ~350 Ma, ~425 Ma, ~600 Ma, 1300 Ma and 1850 Ma (Figure 6b). These data indicate that the basement rocks that were melted contain zircons that are Proterozoic and younger. This indicates that the dacites were the product of melting continental crust, rather than a more juvenile (e.g. ophiolitic) basement.

4.2 Equivalent phases of magmatism

The two samples of dacite that were examined here are similar to those described from Central Sulawesi by Brouwer (1947), and are potentially equivalent to units of the Ongka Volcanics from northern Sulawesi (Polve et al. 1997; van Leeuwen et al. 1994), the Gimpu Volcanics from the neck of Sulawesi (Priadi et al. 1994; Polve et al., 1997) and granites and rhyolites found near Kulawi, central Sulawesi (Priadi et al. 1994). The Kulawi and Gimpu volcanics crystallised between approximately 6 Ma and 2 Ma according to K-Ar data (Priadi et al. 1994), indicating that magmatism was quite widespread in Sulawesi during the Mio-Pliocene.

4.3 Petrogenesis

The presence of hornblende in the Kolaka Dacite indicates that there was a considerable amount of H₂O associated with the generation of the melts. This could be interpreted as volcanics being produced in a subduction setting, where water is driven off subducted oceanic crust, leading to partial melting of the mantle wedge and arc volcanism, particularly as the trace element data have a

subduction signature. However, the subduction signature could also be inherited from remelting an arc-like protolith, and therefore does not necessarily mean that the dacite is the product of melting associated with a subduction zone. Such ideas have been discussed in many of the papers that present geochemical data from Mio-Pliocene rocks of similar composition (Leterrier et al. 1990; Priadi et al., 1994; Polve et al. 1997; Elburg and Foden 1999a; 1999b; Elburg et al., 2002; 2003). We favour a scenario that does not invoke melting associated with a subduction zone as there is no geophysical evidence to support the existence of a subducted slab beneath this part of Sulawesi in the Pliocene (e.g. Hall 2002; 2012; Spakman and Hall 2010). Since Bone Bay was formed by extensional and strike-slip faulting during the Mio-Pliocene (e.g. Camplin and Hall 2013; 2014) it is possible that such movement and an elevated geotherm led to partial melting of the crust, where melts ascended along strike-slip faults, such as the Kolaka Fault.

CONCLUSIONS

Undeformed dacites found north of the Kolaka fault zone on the SE Arm of Sulawesi were emplaced ~4.2 million years ago. Since these rocks are not deformed, these rocks provide a minimum age for the timing of metamorphism of the schist country rock. We suggest that the dacite intrusions were possibly associated with movement along a strand of the Kolaka Fault or intruded along earlier formed foliation planes in the country rock. The intrusions involved entrainment of Miocene to Proterozoic inherited zircon grains and cores due to partial melting of the country rock. These data indicate that the basement of the SE Arm of Sulawesi is continental in origin, rather than ophiolitic.

ACKNOWLEDGEMENTS

Marnie Forster, Pak Musri and Abang (“Ega”) Surya Nugraha are thanked for their help in the field. Christina Manning and Matthew Thirlwall are thanked for providing the major and trace element geochemistry data as well as Inga Sevastjanova for developing code for plotting U-Pb data. We thank the industrial sponsors of the Southeast Asia Research Group consortium for funding this research. We also thank D. Tanner for commenting on an earlier version of this manuscript. Ian Watkinson and Chris Morley are thanked for reviewing the manuscript.

REFERENCES

- Audley-Charles, M.G., 1974. Sulawesi. *Geological Society London Special Publications* **4**, 365–378.
- Berry, R.F., Grady, A.E., 1987. Mesoscopic structures produced by Plio-Pleistocene wrench faulting in South Sulawesi, Indonesia. *Journal of Structural Geology* **9**, 563–571.
- Black, L., Kamo, S., Allen, C., Davis, D., Aleinikoff, J., Valley, J., Mundil, R., Campbell, I., Korsch, R., Williams, I.S., 2004. Improved $^{206}\text{Pb}/^{238}\text{U}$ microprobe geochronology by the monitoring of a trace-element-related matrix effect; SHRIMP, ID-TIMS, ELA-ICP-MS and oxygen isotope documentation for a series of zircon standards. *Chemical Geology* **205**, 115–140.
- Brouwer, H.A., 1947. Geological Exploration of the Island of Celebes, Summary and Results. North-Holland, Amsterdam, pp. 1-64.
- Camplin, D.J., Hall, R., 2013. Insights into the structural and stratigraphic development of Bone Gulf, Sulawesi. *Proceedings Indonesian Petroleum Association, 37th Annual Convention*, IPA13-G-079 1-24.
- Camplin, D.J., Hall, R., 2014. Neogene history of Bone Gulf, Sulawesi, Indonesia. *Marine and Petroleum Geology*, **57**, 88-108

- Cottam, M.A., Hall, R., Forster, M.A., Boudagher-Fadel, M.K., 2011. Basement character and basin formation in Gorontalo Bay, Sulawesi, Indonesia: new observations from the Togian Islands. In: Hall, R., Cottam, M. A. & Wilson, M. E. J. (Eds.), *The SE Asian gateway: history and tectonics of Australia-Asia collision*. Geological Society of London Special Publication, 355, 177-202.
- Elburg, M., Foden, J., 1999a. Sources for magmatism in Central Sulawesi: geochemical and Sr–Nd–Pb isotopic constraints. *Chemical Geology* **156**, 67–93.
- Elburg, M.A., Foden, J., 1999b. Geochemical response to varying tectonic settings: An example from southern Sulawesi (Indonesia). *Geochimica et Cosmochimica Acta* **63**, 1155–1172.
- Elburg, M., van Leeuwen, T., Foden, J., Muhardjo, 2003. Spatial and temporal isotopic domains of contrasting igneous suites in Western and Northern Sulawesi, Indonesia. *Chemical Geology* **199**, 243–276.
- Elburg, M.A., van Leeuwen, T., Foden, J., 2002. Origin of Geochemical Variability by Arc–Continent Collision in the Biru Area, Southern Sulawesi (Indonesia). *Journal of Petrology* **43**, 581–606.
- Hall, R., 1996. Reconstructing Cenozoic SE Asia. *Geological Society London Special Publications* **106**, 153-184.
- Hall, R., 2002. Cenozoic geological and plate tectonic evolution of SE Asia and the SW Pacific: computer-based reconstructions, model and animations. *Journal of Asian Earth Sciences* **20**, 353–431.
- Hall, R., 2012. Late Jurassic–Cenozoic reconstructions of the Indonesian region and the Indian Ocean. *Tectonophysics* **570-571**, 1–41.
- Hamilton, W., 1979. Tectonics of the Indonesian region. USGS Professional Paper **1078**, 345 pp.
- Jaya, A., Nishikawa, O., 2013. Paleostress reconstruction from calcite twin and fault-slip data using the multiple inverse method in the East Walanae fault zone: Implications for the Neogene contraction in South Sulawesi, Indonesia. *Journal of Structural Geology* **55**, 34–49.

- Katili, J.A., 1970. Large transcurrent faults in Southeast Asia with special reference to Indonesia. *Geologische Rundschau* **59**, 581–600.
- Katili, J.A., 1978. Past and present geotectonic position of Sulawesi, Indonesia. *Tectonophysics* **45**, 289–322.
- Le Bas, M.J., Streckeisen, A.L., 1991. The IUGS systematics of igneous rocks. *Journal of the Geological Society* **148**, 825–833.
- Letierrier, J., Yuwono, Y.S., Soeria-Atmadja, R., Maury, R.C., 1990. Potassic volcanism in central Java and south Sulawesi, Indonesia. *Journal of Southeast Asian Earth Sciences* **4**, 171–187.
- Ludwig, K.R., 2003. *User's Manual for Isoplot 3.00: A Geochronological Toolkit for Microsoft Excel*. Berkeley Geochronology Centre Special Publication.
- Muir, R.J., Ireland, T.R., Weaver, S.D., Bradshaw, J.D., 1996. Ion microprobe dating of Paleozoic granitoids: Devonian magmatism in New Zealand and correlations with Australia and Antarctica. *Chemical Geology* **127**, 191–210.
- Palme, H., O'Neill, H.S.C., 2003. Cosmochemical estimates of mantle composition. *Treatise on Geochemistry* **2**, 1–38.
- Parkinson, C., 1998a. Emplacement of the East Sulawesi Ophiolite: evidence from subophiolite metamorphic rocks. *Journal of Asian Earth Sciences* **16**, 13–28.
- Parkinson, C., 1998b. An outline of the petrology, structure and age of the Pompangeo Schist Complex of central Sulawesi, Indonesia. *Island Arc* **7**, 231–245.
- Polve, M., Maury, R.C., Bellon, H., Rangin, C., Priadi, B., Yuwono, S., Joron, J.L., Atmadja, R.S., 1997. Magmatic evolution of Sulawesi (Indonesia): constraints on the Cenozoic geodynamic history of the Sundaland active margin. *Tectonophysics* **272**, 69–92.
- Priadi, B., Polve, M., Maury, R.C., Bellon, H., Soeria-Atmadja, R., Joron, J.L., Cotten, J., 1994. Tertiary and Quaternary magmatism in Central Sulawesi: chronological and petrological constraints. *Journal of Southeast Asian Earth Sciences* **9**, 81–93.

- Rusmana, E., Sukido, D., Sukarna, E., Haryono, Simandjuntak, T.O., 1993. *Geological report of the Lasusua and Kendari Sheets, Sulawesi*. Geological Research and Development Centre, Bandung, Scale 1:250,000.
- Sambridge, M.S., Compston, W., 1994. Mixture modeling of multicomponent data sets with application to ion-probe zircon ages. *Earth and Planetary Science Letters* **128**, 373-390.
- Silver, E.A., McCaffrey, R., Joyodiwiryo, Y., Stevens, S., 1983a. Ophiolite emplacement by collision between the Sula Platform and the Sulawesi island arc, Indonesia. *Journal of Geophysical Research* **88**, 9419-9435.
- Silver, E.A., McCaffrey, R., Smith, R.B., 1983b. Collision, rotation, and the initiation of subduction in the evolution of Sulawesi, Indonesia. *Journal of Geophysical Research* **88**, 9407-9418.
- Simandjuntak, T.O., Surono and Sukido., 1984. *Geological Report of the Kolaka Quadrangle, Sulawesi, Scale 1:250,000*. Open file report, Indonesian Geological Research and Development Centre, Bandung, 50 p.
- Simandjuntak, T.O., Surono, Sukido, 1994. *Geological Map of the Kolaka Quadrangle, Sulawesi*. Geological Research and Development Centre, Bandung, Scale 1:250,000.
- Spakman, W., Hall, R., 2010. Surface deformation and slab--mantle interaction during Banda arc subduction rollback. *Nature Geoscience* **3**, 562-566.
- Sukamto, R., 1982. *The Geology of the Pangkajene and Western Part of Watampone, Sulawesi*. Geological Research and Development Centre, Bandung, Quadrangles Series, scale 1:250,000.
- Sukamto, R., Simandjuntak, T.O., 1983. Tectonic relationship between geologic provinces of western Sulawesi, Eastern Sulawesi and Banggai-Sula in the light of sedimentological aspects. *Bulletin of the Geological Research and Development Centre* **7**, 1-12.
- Surono, 1994. Stratigraphy of the southeast Sulawesi continental terrane, Eastern Indonesia. *Journal of Geology and Mineral Resources* **4**, 4-11.

- Surono, 1998. Geology and origin of the southeast Sulawesi continental terrane, Indonesia. *Media Teknik* **3**, XX. Republished in Surono. Geology of the southeast Arm of Sulawesi. *Journal of Geological Resources Special Publication* **35**, 13-31.
- van Leeuwen, T.M., 1981. The geology of southwest Sulawesi with special reference to the Biru area. The geology and Tectonics of Eastern Indonesia, *Geological Research and Development Centre Special Publication* **2**, 277–304.
- van Leeuwen, T.M., Taylor, R., Coote, A., Longstaffe, F.J., 1994. Porphyry molybdenum mineralization in a continental collision setting at Malala, northwest Sulawesi, Indonesia. *Journal of Geochemical Exploration* **50**, 279–315.
- van Leeuwen, T.M., Allen, C.M., Kadarusman, A., Elburg, M., Michael Palin, J., Muhardjo, Suwijanto, 2007. Petrologic, isotopic, and radiometric age constraints on the origin and tectonic history of the Malino Metamorphic Complex, NW Sulawesi, Indonesia. *Journal of Asian Earth Sciences* **29**, 751–777.
- Wakita, K., Sopaheluwakan, J., Miyazaki, K., Zulkarnain, I., 1996. Tectonic evolution of the Bantimala complex, south Sulawesi, Indonesia. *Geological Society London Special Publications* **106**, 353–364.
- White, L.T., Ahmad, T., Ireland, T.R., Lister, G.S., Forster, M.A., 2011. Deconvolving episodic age spectra from zircons of the Ladakh Batholith, northwest Indian Himalaya. *Chemical Geology* **289**, 179–196.
- White, L.T., Ireland, T.R., 2012. High-uranium matrix effect in zircon and its implications for SHRIMP U–Pb age determinations. *Chemical Geology* **306-307**, 78-91.

Figure Captions

Figure 1. Map showing the location of major faults and geological terranes of Sulawesi. The focus of this study is on dacites found within a strand of the Kolaka fault zone (modified after Cottam et al. 2011).

Figure 2. Regional geology map showing the position of the Kolaka Fault and where samples ES12-21 and ES12-22 were collected. The geological boundaries were modified from Simandjuntak et al., (1994) and the structural lineaments (black lines) were derived from an interpretation of Shuttle Radar Topographic Mission (SRTM) data.

Figure 3. Photographs of a road-cutting where dacite was found to intrude schist, (a) looking to the NE, and (b) towards SW. Sample ES12-22 was collected at this exposure. The contact between the schist and the dacite is steep (b-c), and (c) is ultimately controlled by the orientation of the existing foliation in the schist. The dacite is (c) fractured by sub-horizontal cooling joints; it is (d) fine-grained with large crystals of hornblende and felsic xenoliths, and (e) predominantly has steep flow banding.

Figure 4. Thin sections of the dacite show that it is (a) relatively fine-grained and porphyritic, composed of dominantly plagioclase, quartz and hornblende, as well as biotite (although less abundant). Thin sections also show that (b) the centimetre scaled hornblende crystals that were observed in hand specimen are in fact clusters of smaller hornblende crystals (glomerocrysts). These were observed to be (c) altered on several occasions. Each microphotograph that is shown here, shows the sample in plane polarised light. Sample ES12-22 is shown in (a), and sample ES12-21 is shown in (b) and (c).

Figure 5. (a-b). The results of whole-rock, major trace element analyses for samples ES12-21 and ES12-22 were plotted on (a) a total alkali ($\text{Na}_2\text{O} + \text{K}_2\text{O}$) vs silica (SiO_2) (TAS) diagram. This shows that both samples have very similar compositions and plot within the dacite field. The trace element data were normalised to an average primitive mantle composition (Palme and O'Neill, 2003) and (b) plotted on a spider diagram. This shows that all element are enriched relative to an average primitive mantle composition. The relative enrichment in Pb and Sr, and relative depletion of Nb, Nd, Y and Yb could be interpreted as a subduction signature.

Figure 6. U-Pb age data of ES12-21 and ES12-22 were combined because both samples yielded very similar results and the composition and mineralogy of the samples were essentially the same. The combined data is shown here on (a-c) relative probability/frequency plots covering different periods of geological time. Many of the analyses of zircon grains and zircon rims were (a) <8 Ma age, and this population was interpreted to mark the approximate timing of intrusion. Analyses that were (b) >8 Ma were interpreted to represent inheritance. This interpretation was cross-checked with CL images of the zircon morphology (Supplementary File 2). As we could not distinguish one dominant age from the <8 Ma population, we followed the same approach as shown in White et al. (2011) using the “unmix age” function within Isoplot (Ludwig 2003) to (c) calculate the age of each population defined on a relative probability plot.

Table Captions

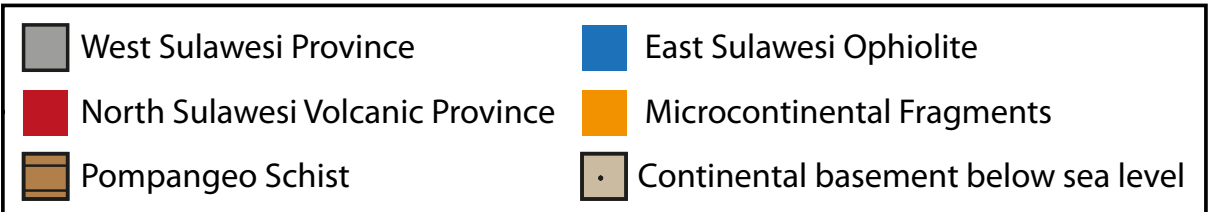
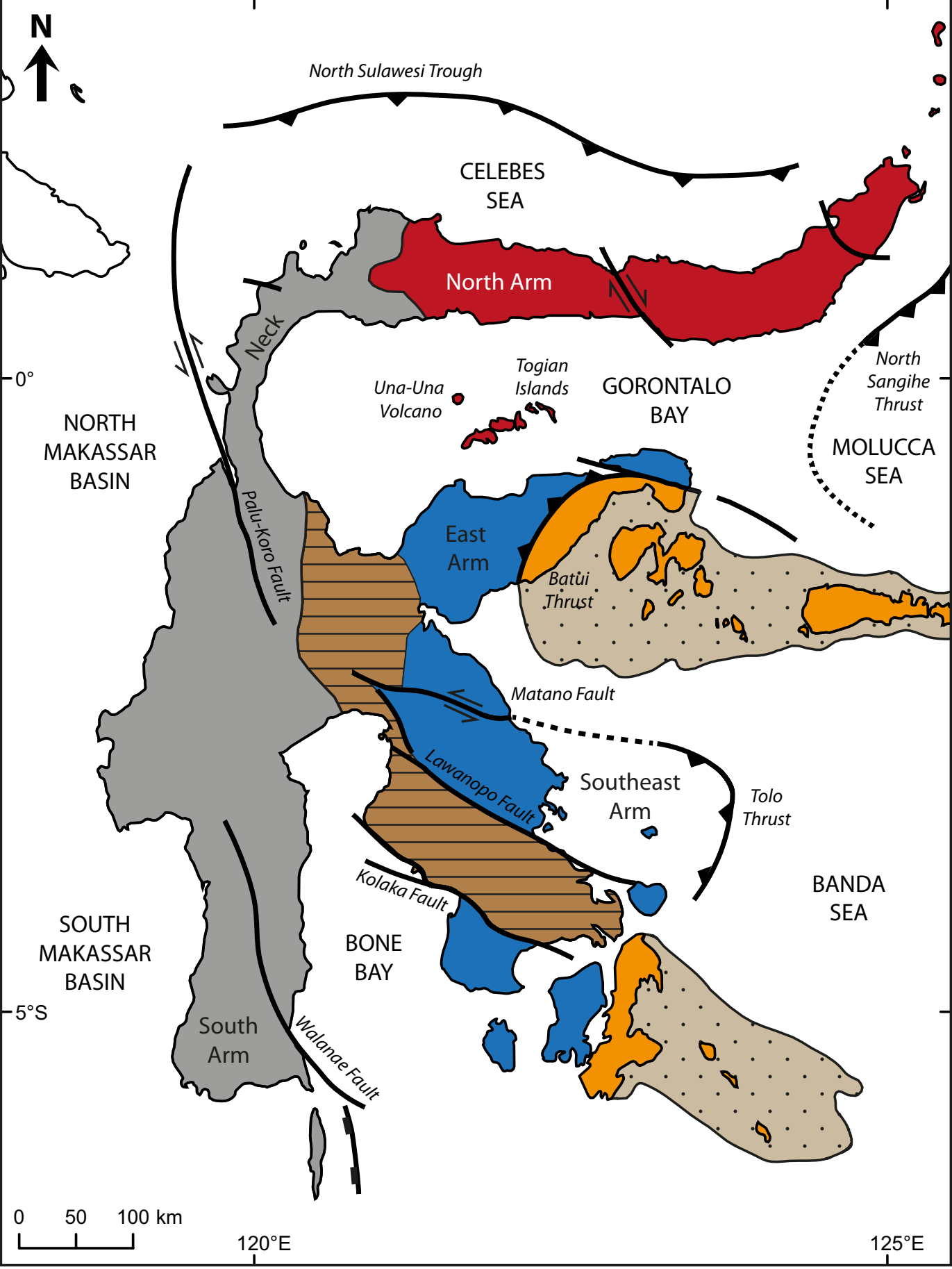
Table 1. Whole rock major and trace element data for samples ES12-21 and ES12-22.

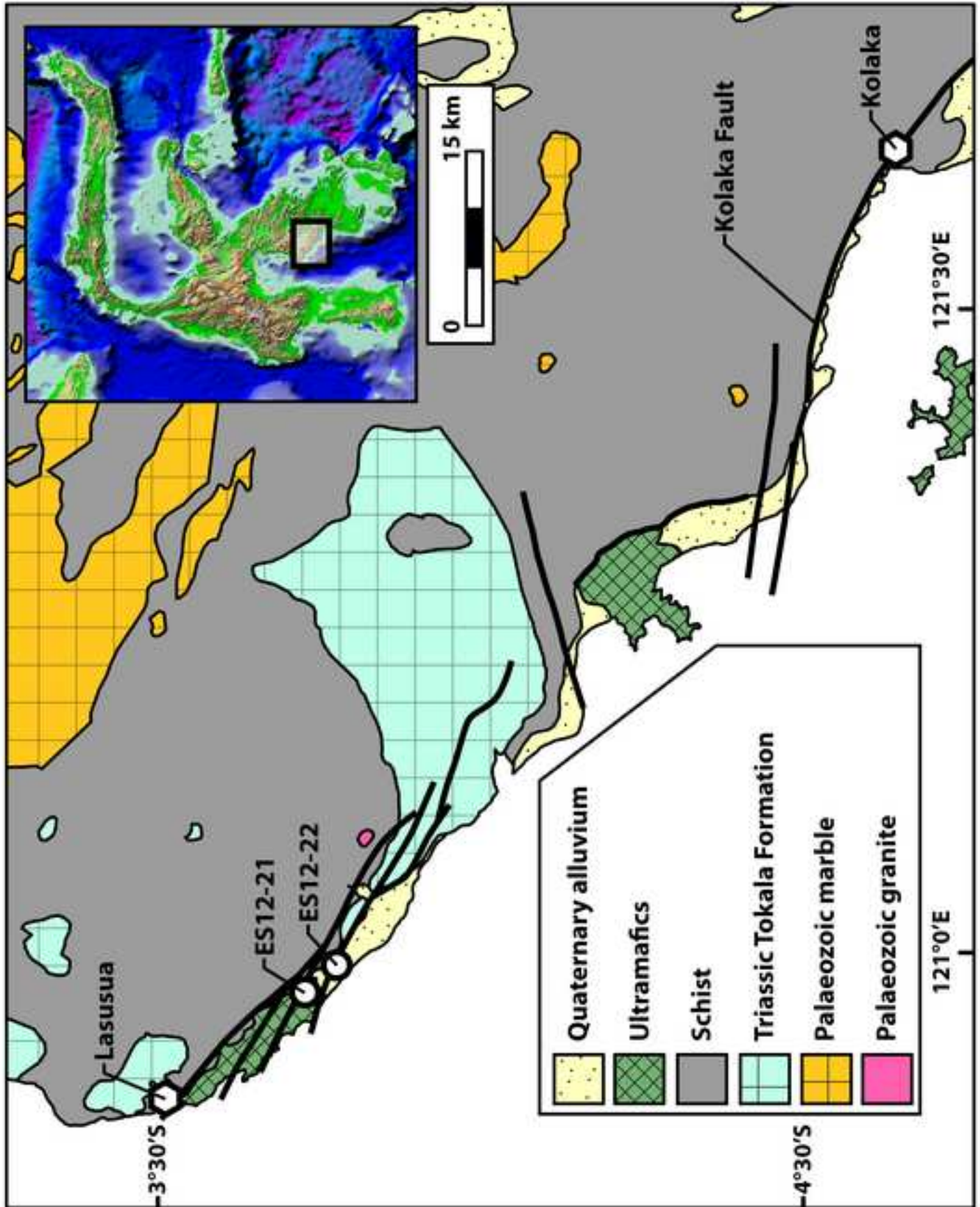
Supplementary Data

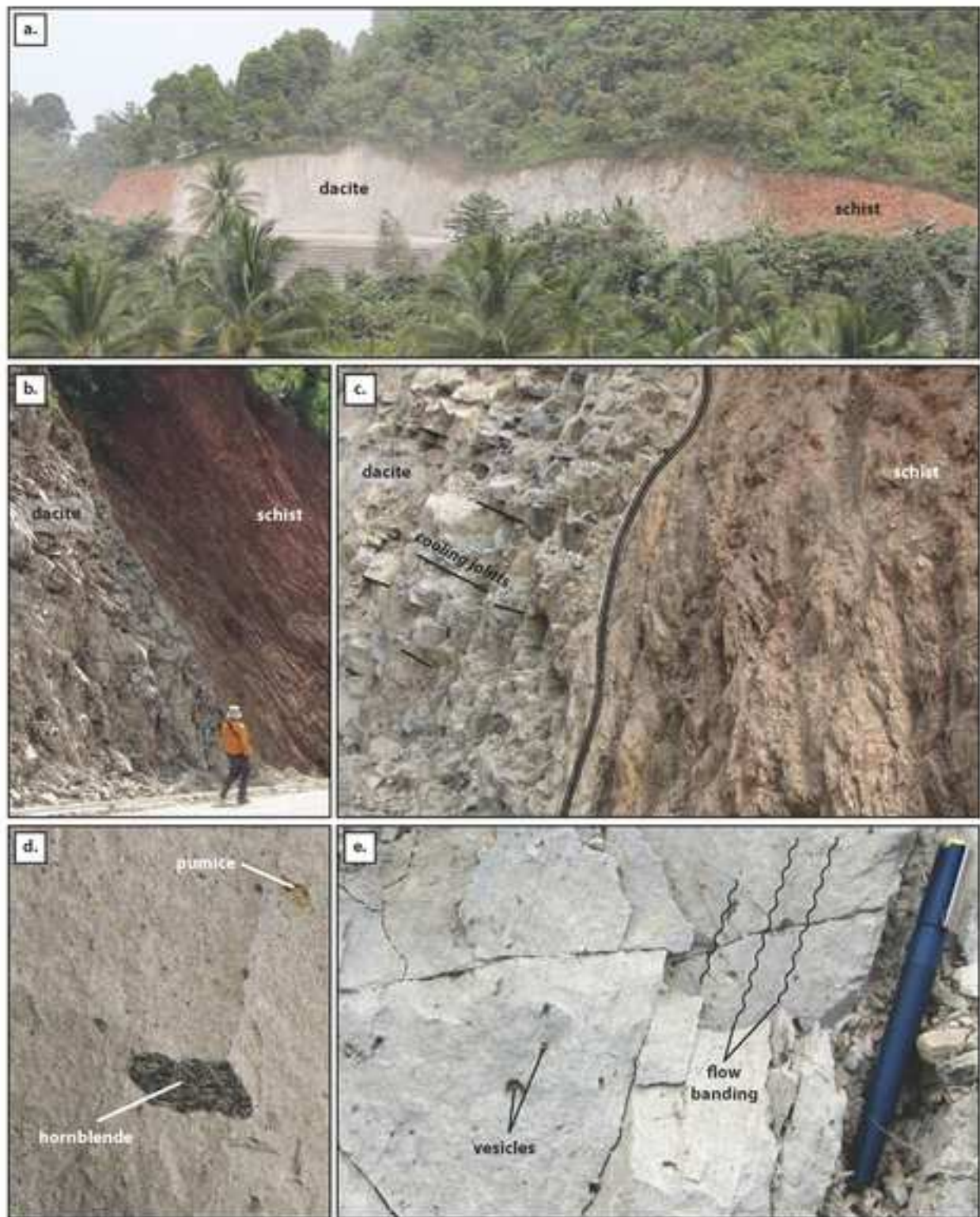
Supplementary File 1: Summary of SHRIMP U-Pb data collected from samples (a) ES12-21 and (b) ES12-22.

Supplementary File 2: Scanning electron microscope cathodoluminescence (CL) images of the zircons from samples ES12-21 and ES12-22 and the location of SHRIMP ablation pits.

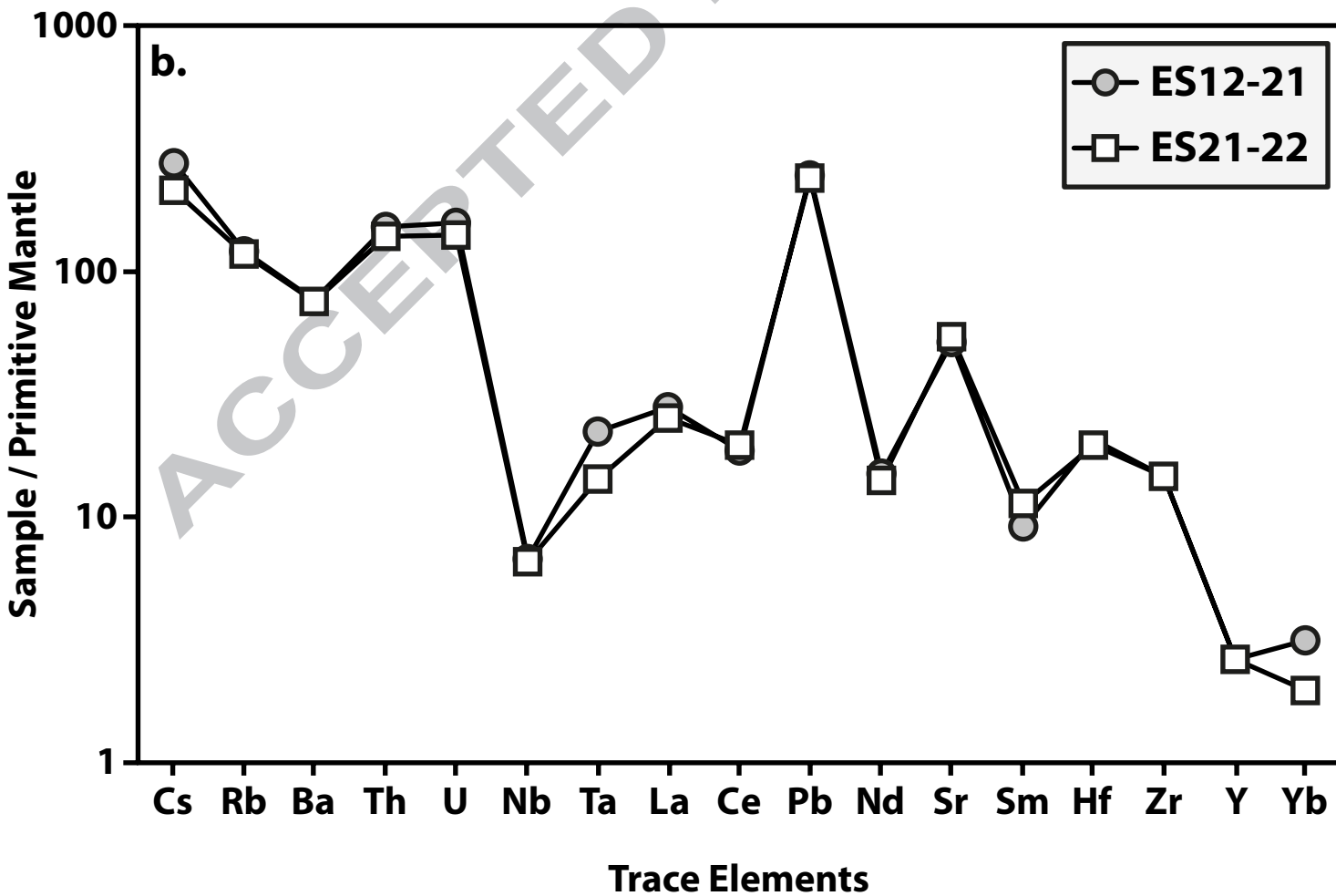
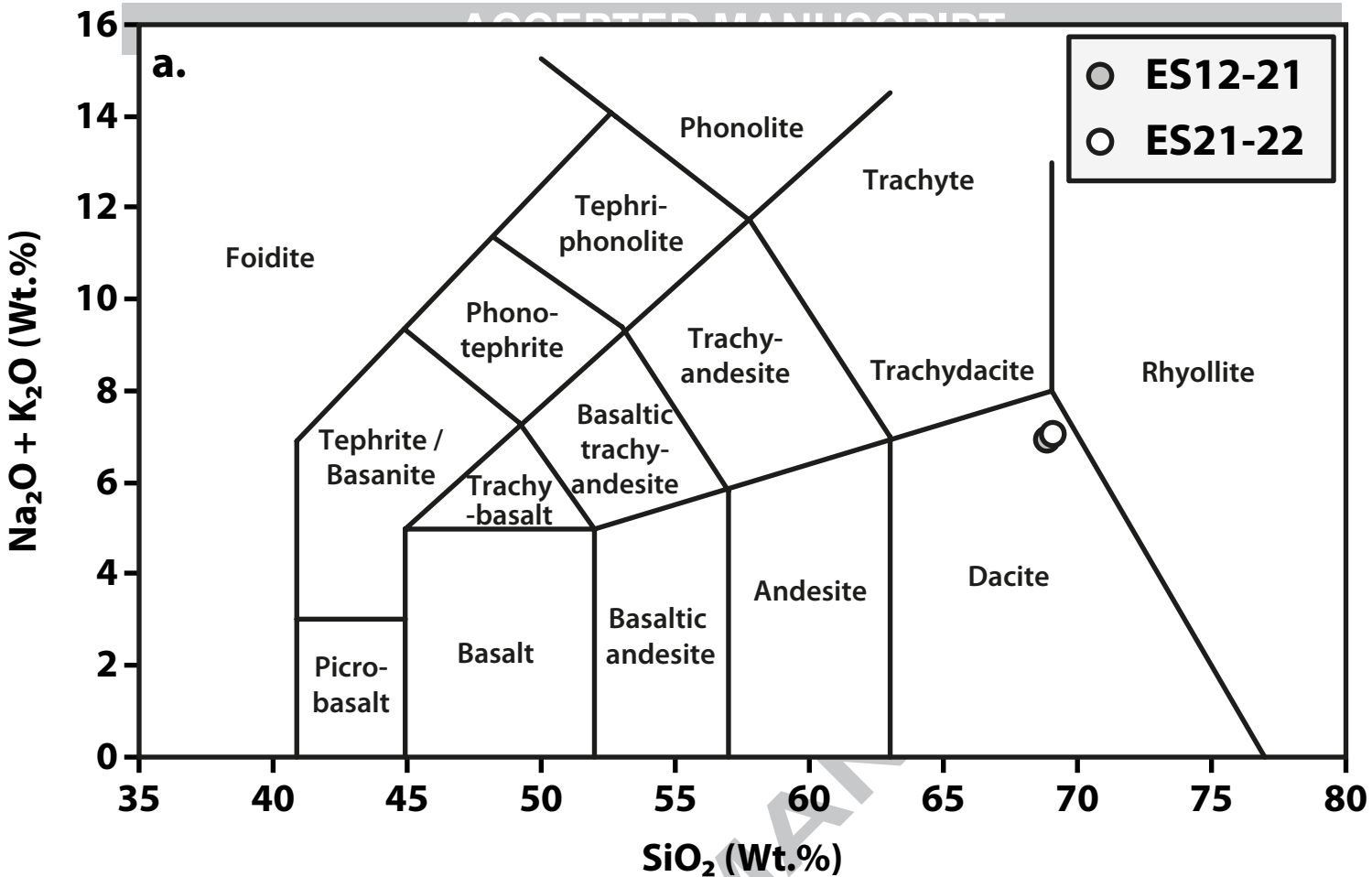
Supplementary File 3: A uranium concentration vs. apparent age plot of the SHRIMP results obtained from zircons that were <10 Ma shows that there is no correlation between an increase in uranium concentration and apparent age (cf. White and Ireland 2012). This indicates that there is no observable matrix effect associated with the SHRIMP measurements of the zircons analysed in this study.











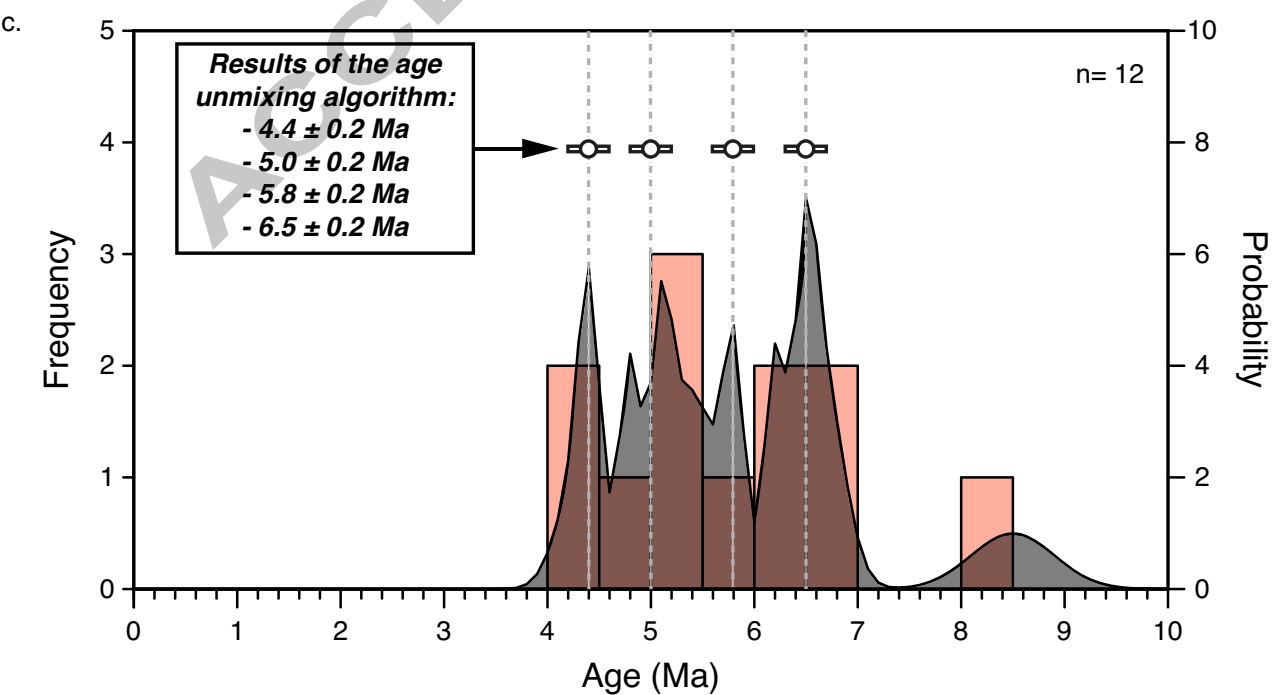
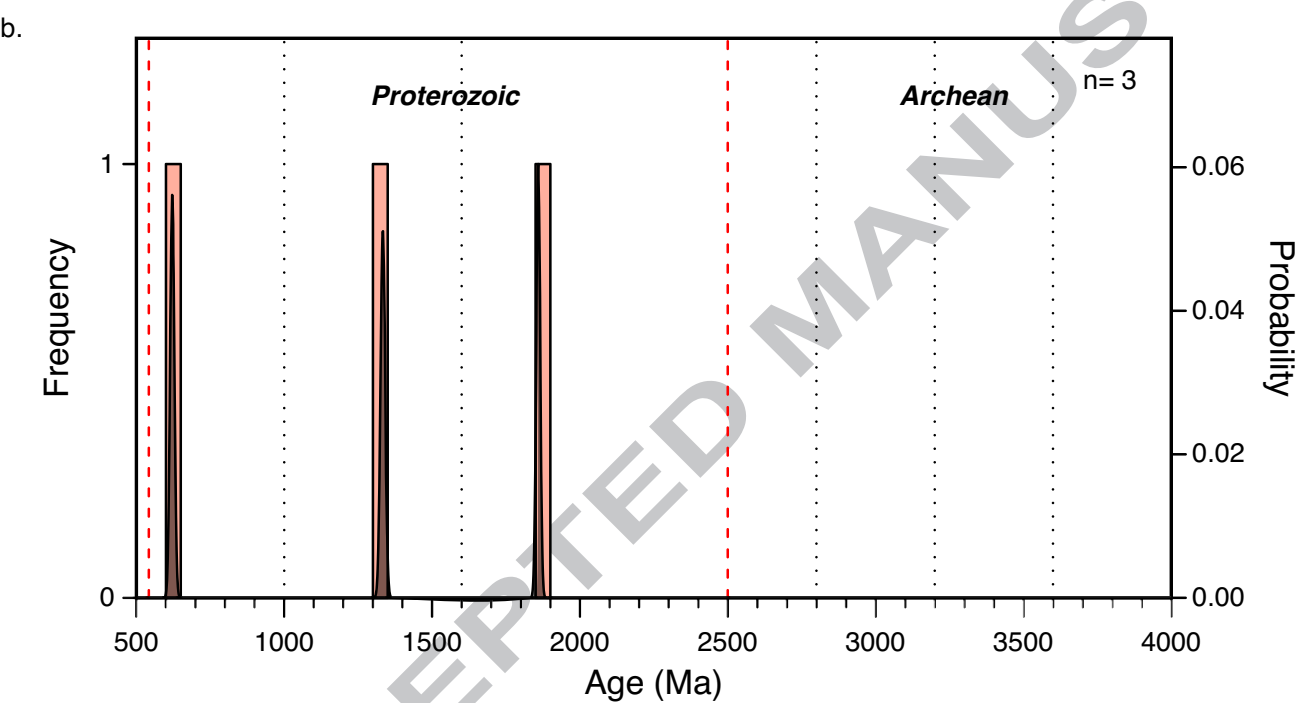
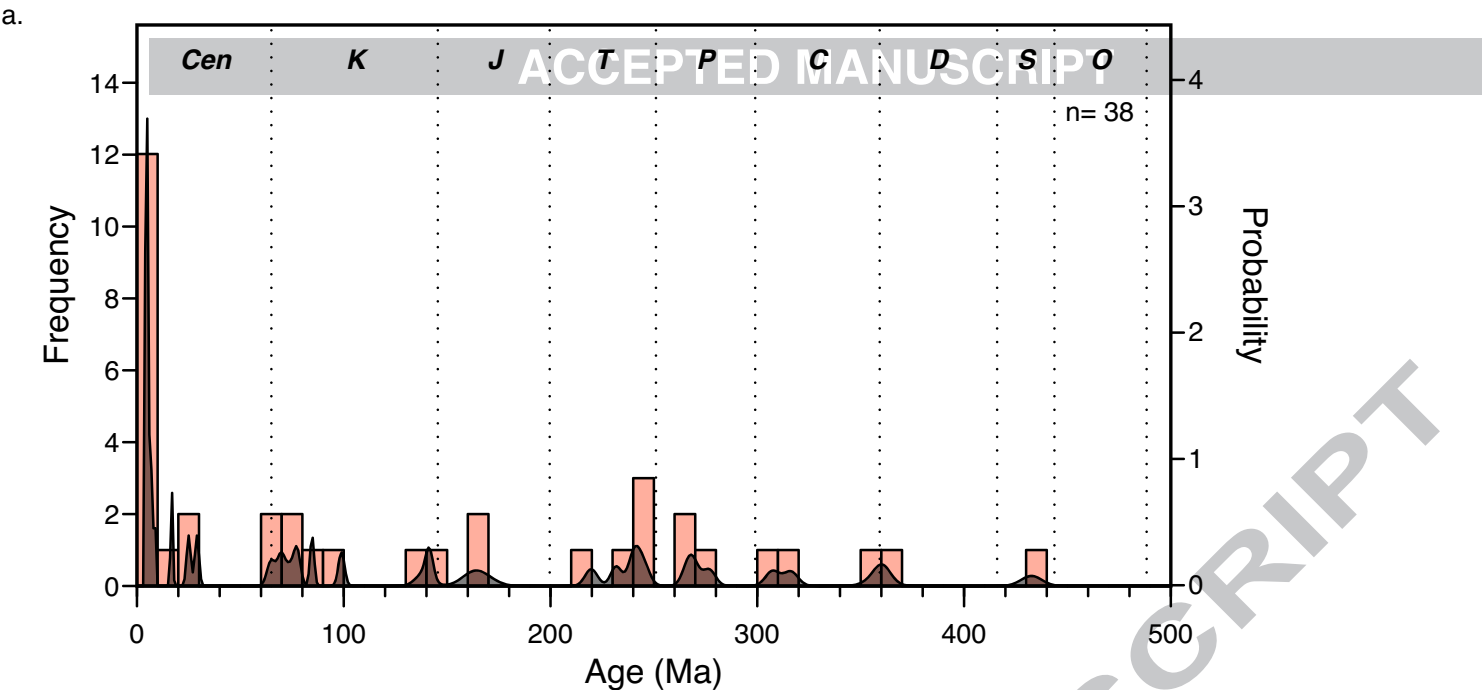


Table 1: Whole rock major and trace element geochemistry results of the Kolaka Dacite

	ES12-21	ES21-22
SiO ₂ (wt.%)	68.87	69.09
Al ₂ O ₃ (wt.%)	15.06	14.99
Fe ₂ O ₃ (wt.%)	2.40	2.49
MgO (wt.%)	1.86	1.93
CaO (wt.%)	3.24	3.44
Na ₂ O (wt.%)	3.66	3.85
K ₂ O (wt.%)	3.280	3.209
TiO ₂ (wt.%)	0.489	0.494
MnO (wt.%)	0.036	0.041
P ₂ O ₅ (wt.%)	0.137	0.164
SO ₃ (wt.%)	0.000	0.000
Ni (ppm)	45.0	46.4
Co (ppm)	12.8	8.5
Cr (ppm)	71.7	89.2
V (ppm)	44.8	45.3
Sc (ppm)	6.2	6.1
Cu (ppm)	20.9	20.0
Zn (ppm)	51.4	47.0
As (ppm)	1.2	1.7
S (ppm)	38	41
F (ppm)	460	580
Cl (ppm)	137	76
Br (ppm)	0.4	0.3
Ga (ppm)	20.3	20.1
Pb (ppm)	45.1	44.4
Sr (ppm)	1050.2	1100.0
Rb (ppm)	73.2	71.2
Ba (ppm)	513.7	511.5
Zr (ppm)	158.9	158.7
Nb (ppm)	4.0	3.9
Ta (ppm)	0.9	0.6
Mo (ppm)	-0.1	0.0
Th (ppm)	12.6	11.5
U (ppm)	3.4	3.1
Y (ppm)	11.5	11.5
La (ppm)	19.2	17.3
Ce (ppm)	33.3	35.0
Nd (ppm)	19.8	18.7
Sm (ppm)	3.9	4.9
Yb (ppm)	1.5	0.9
Hf (ppm)	6.2	5.9
Cs (ppm)	5	4
LOI (wt.%)	0.89	0.61
Sum of Major Elements (wt.%)	99.04	99.70
Sum of Trace Elements (ppm)	0.33	0.34
Total (wt.%)	99.37	100.04

Research Highlights

- We report on previously undocumented dacite bodies in SE Sulawesi
- The dacite is undeformed and found within the Kolaka strike-slip fault zone
- U/Pb SHRIMP dating of zircons indicates dacite emplacement at 4.2 Ma
- Inherited ages indicate the dacite melted continental, rather than ophiolitic basement

ACCEPTED MANUSCRIPT